Life Sciences 222 (2019) 94–102

Contents lists available at ScienceDirect

Life Sciences

journal homepage: www.elsevier.com/locate/lifescie

Targeting of Thymoquinone-loaded mesoporous silica nanoparticles to different brain areas: In vivo study☆

Heba M. Fahmy, Mohamed M. Fathy*, Raghda A. Abd-elbadia, Wael M. Elshemey

Biophysics Department, Faculty of Science, Cairo University, 12613 Giza, Egypt

ARTICLE INFO

Keywords:
Mesoporous silica nanoparticles
Thymoquinone
Oxidative stress
Biodistribution
Brain, rats

ABSTRACT

Aims: Drug delivery to the brain is hindered by the blood-brain-barrier (BBB) that filters out most of drugs after systemic administration. Therefore, there is an urgent need to develop more efficient drug delivery systems to deliver pharmaceuticals to brain. In this work, the distribution and the effect of Thymoquinone (TQ) on different oxidative stress biomarkers in different brain areas, either in the free form or encapsulated in mesoposrous silica nanocarriers (MSNs) were systematically studied.

Materials and methods: MSNs and Thymoquinone-loaded mesoporous silica nanoparticles (MSN-TQ) were prepared and characterized using TEM, DLS, and zeta potential. The encapsulation efficiency and release profile of MSN-TQ were investigated as well. The chromatographic quantification of TQ was carried out to evaluate the effect of TQ loading in MSNs on the TQ distribution throughout different brain regions. Additionally, some oxidative stress biomarkers were evaluated like: glutathione reduced (GSH), glutathione-s-transferase (GST), nitric acid (NO) and malondialdehyde (MDA).

Key findings: Results showed that the encapsulation of TQ in MSNs enhanced its delivery to some brain areas (cortex, thalamus, hypothalamus and midbrain), on the other hand it reduced its delivery to the cerebellum while its delivery to medulla and striatum was not changed compared to free TQ. Neither free TQ nor MSN-TQ were able to reach the hippocampus.

Significance: It was found that the encapsulation of TQ in MSNs resulted in its redistribution in different brain areas, thus, MSNs could be potentially utilized as a drug delivery system for selectively targeting the drug to certain brain areas.

1. Introduction

The delivery of most Central Nervous System (CNS) active drugs, especially, biopharmaceuticals is potentially hindered by the Blood Brain Barrier (BBB).The BBB not only limits the passage of potentially harmful chemicals into the brain, but also limits the delivery of beneficial drugs [1]. Moreover, it has been noticed that over 60% of novel drugs are water insoluble in the development stage. Thus, the improvement of drug solubility and thereby its bioavailability are among the most challenging prospects of the drug development process. In the last few years, increasing attention has been devoted toward the development of novel drug delivery systems that can enhance drug bioavailability [2,3].

Mesoporous silica nanoparticles (MSNs) are excellent matrices for molecules and biomolecules anchorage, making these materials very promising for several industrial applications, chemical and environmental engineering, medicine and biology. Thousands of studies reported MSNs properties and formations, due their strong suitability for applications in many fields such as adsorption, separation, catalysis and advanced materials. The control of particle size, morphology and porosity, advancements in the synthesis of mesoporous silica materials along with their chemical stability, have made silica matrices highly attractive as the structural basis for a wide variety of applications [4]. These reasons make MSNs one of the most used Nano-carriers that are suitable for delivery of drugs [5], proteins [5], vitamins [6], and antioxidants [7]. A study conducted by **Baghirov *et al.*** proved that spherical and rod-shaped MSNs with the smallest dimension in the 100 nm range either coated or not with copolymers were able to cross the BBB [8].

Thymoquinone (TQ) is the main constituent of the volatile oil of *Nigella sativa seeds*. The volatile oil of *Nigella sativa* was shown to contain 24% TQ [9]. TQ protects organs against oxidative damage induced

☆ This manuscript was written with contributions from all authors.

* Corresponding author at: Biophysics Department, Faculty of Science, Cairo University, Giza, Egypt.
E-mail address: mfathy@sci.cu.edu.eg (M.M. Fathy).

https://doi.org/10.1016/j.lfs.2019.02.058
Received 16 October 2018; Received in revised form 21 February 2019; Accepted 27 February 2019
Available online 01 March 2019
0024-3205/

by a variety of free radical generating pathologies [10]. It also acts as anti-inflammatory [11], neuroprotective [12,13], and anticancerous drug [14,15]. Despite that TQ has tremendous potential as a therapeutic compound, it has a toxic effect if it is taken in large amounts [16]. Moreover, its potency and bioavailability is limited by poor solubility and poor formulation characteristics of its high lipophilicity. Thus, using a suitable Nano-carrier will greatly improve its pharmacokinetics and pharmacodynamics.

Compared to other organs, the brain is the most exposed organ to free radicals. This is because, to supply energy to its areas, human brain cells utilize 20% of the oxygen consumed by the body while it constitutes only 2% of the body weight. Exposure of the brain to free radicals is also enhanced by its high levels of polyunsaturated fatty acids, which are regarded as a good target for lipid peroxidation [17,18]. Moreover, the brain has an abundance of redox-active transition metal ions in addition to the relative reduction of its antioxidant defense systems [19].

Lately, there has been a growing interest in examining the possibility of drug delivery to brain using drug carriers [20–22]. Unfortunately, there is no study that examined the effect of drug loading on carriers on the distribution of drugs in different brain areas. Hence, this work aims to quantitatively evaluate the effect of TQ loading in MSNs on the TQ distribution in different brain regions compared to free TQ. In addition, this work focuses on examining the oxidative stress condition of different rat brain areas after being treated with free TQ, MSNs or MSN-TQ.

2. Materials and methods

2.1. Materials

Tetraethyl Orthosilicate (TEOS, 99%), Cetyltrimethylammonium Bromide (CTAB) (99%), Thymoquinone (2-isopropyl-5-methyl-1, 4-benzoquinone), 99% Ethanol, Dimethyl Sulfoxide (DMSO) and 1-Chloro-2, 4 Dinitrobenzene (CDNB) 30 mmol/l were purchased from Sigma–Aldrich (St. Louis, MO, USA). 2-ethoxyethanol ($C_2H_5OCH_2CH_2OH$, 99%) was purchased from Merck. Ammonia hydroxide (NH_4OH, 28%) was purchased from Fluka. Thiobarbituric acid (TBA) and 98% reduced glutathione were purchased from Sigma Aldrich, Germany. Phosphate buffered saline (PBS) was obtained from the Bio Basic Inc. USA. 1-chloro-2, 4 dinitrobenzene (CDNB) was purchased from Sigma Aldrich, St. Louis, USA. 98% Trichloroacetic acid (TCA) was obtained from SDFCL, Egypt.

Potassium phosphate buffer, *Phosphate-buffered saline* (PBS) pH 7.4 (100 mM/l), Potassium dihydrogen phosphate buffer and kits for the determination of oxidative stress biomarkers: Glutatione reduced (GSH), Nitric oxide (NO), No. GR 25 11 and NO 25 33, respectively were purchased from Bio Diagnostic Co., Giza, Egypt.

2.2. Preparation methods

2.2.1. Preparation of mesoporous silica nanoparticles (MSNs)

MSNs were synthesized according to the method given by El bialy et al. [23]. Briefly, 0.5 g of CTAB (cationic surfactant) was dissolved in 70 ml of deionized water using a magnetic stirrer until a clear solution was obtained. Then, 0.5 ml of ammonium hydroxide (28%) and 30 ml of the co-solvent (2-ethoxyethanol) were added to the CTAB solution. The mixture was strongly stirred in a closed flask at room temperature for 30 min. After that, 2.5 ml of TEOS was added into the mixture and vigorously stirred for 24 h. The prepared silica was collected using centrifugation at 6000 rpm for 20 min, washed 5 times with ethanol and then 5 times with deionized water. To ensure complete removal of CTAB, the prepared sample was heated to 500 °C for 6 h.

2.2.2. Preparation of Thymoquinone-loaded mesoporous silica nanoparticles (MSN-TQ)

Thymoquinone (14 mg) was dissolved in 1 ml of DMSO: saline solution with a ratio of 1: 9, respectively. Then, the prepared TQ was added to the MSNs dissolved in deionized water with a weight ratio of 1:1. This suspension was shaken (100 rpm) in a water bath at room temperature for 24 h. After that, MSN-TQ was separated using a centrifuge. The concentration of the free TQ in the supernatant was calculated from a calibration curve, at wave length λ = 253 nm, using a spectrophotometer and the encapsulation efficiency was calculated from the following equation:

$$EE\% = \left(\frac{(total\ drug - free\ drug)}{total\ drug}\right)x100$$

2.3. Physical characterization of the prepared nanoparticles

2.3.1. Transmission electron microscopy (TEM)

TEM permits one to view each individual particle, giving information about the shape and size of the prepared nanoparticles. MSNs morphology and size were determined using TEM (JEM 1230 electron microscope Jeol, Tokyo, Japan). Briefly, a solution of MSNs in deionized water was dropped on a copper coated with carbon grid and the excess sample was drawn off with filter paper. The grid was left 5 min to dry at room temperature prior to the beginning of the examination.

2.3.2. Dynamic light scattering (DLS)

The hydrodynamic mean diameter and size distribution of MSNs and MSN-TQ were determined using the Zetasizer (Nano ZS, Malvern Instruments, UK). Zetasizer detects the scattered laser-light, at an angle of 90° and at a temperature of 25 °C for diluted samples using laser diffraction technique. DLS provides information about the polydispersity of the sample via a Polydispersity Index (PDI). PDI > 0.5 indicates an inhomogeneous particle size distribution [24].

2.3.3. Zeta potential (ZP)

The surface charge of MSNs and MSN-TQ were examined by Zetasizer (Nano ZS, Malvern Instruments, Malvern, UK), at room temperature. ZP values were obtained by measuring the electro-phoretic mobility of the particles moving into the applied electric field.

2.3.4. The absorption spectra of free TQ, MSNs and MSNs-TQ

The absorption spectra of MSN-TQ and TQ were measured using a UV–Vis spectrophotometer (Jenway UV-6420; Barloworld scientific, Essex, UK) in the wavelength range from 200 to 300 nm.

2.3.5. In vitro drug release

In vitro TQ release profiles from MSN-TQ were determined using a dialysis bag diffusion technique. Sterilized dialysis bags with a dialyzer molecular-weight cutoff of 12,000 DA were used to perform the release experiment. These bags were soaked overnight in the release medium. PBS solution of pH 7.4 was used as the drug release media to simulate normal blood/tissue environment. 5 ml of MSN-TQ was centrifuged and redispersed into 5 ml of release media and placed into the dialysis bags. The sealed dialysis bags were placed into bottles, and 15 ml of release media was added to each bottle. These bottles were shaken at a speed of 100 rpm at 37 °C. 2 ml of the external medium was taken from the middle of the beaker and replaced with fresh medium to ensure the sink condition at specified time intervals (0.5, 1, 2, 3, 4, 5, 6, 24 and 48 h). The concentrations of the released TQ were calculated from the calibration curve using a UV–Vis Spectrophotometer at 253 nm (Jenway UV-6420; Barloworld scientific, Essex, UK).

2.4. In vivo experiments

2.4.1. Animals

Male Wistar rats, 6–8 weeks of age and a mean weight of 110 ± 10 g were used in this study. The animals were kept under fixed housing conditions (12 h light/dark cycles) and temperature (25 ± 1 °C). All animals received humane care in compliance with the guidelines of the Ethical Committee of National Research Center, Egypt and the recommendation of Institutional Animal Care and Use Committee, Cairo University with approval number: CUIS 2 16.

2.4.2. Experimental design

Twenty four rats were randomly divided into 4 groups (each of 6 rats) and received a daily intraperitoneal (IP) injection for 5 days as follows: (1) first group (control group): animals were injected with saline and DMSO (10% DMSO: 90% saline), (2) second group (MSNs group): animals were injected with MSN_S (20 mg/kg), (3) third group (TQ group): animals were injected with free TQ (20 mg/kg) and (4) fourth group: (MSN-TQ group) animals were injected with MSN-TQ (20 mg of TQ/kg to 20 mg of MSNs/kg). The duration of the experiment and the doses of TQ were chosen according to the study of Sheikhbahaei et al. (2016) [25].

2.4.3. Handling of tissue samples

Both treated and control animals were sacrificed by sudden decapitation on the 6th day of the experiment. The brain of each animal was quickly removed and rapidly transmitted to an ice-cold Petri dish and dissected to obtain the brain areas (cerebellum, hippocampus, thalamus, cortex, hypothalamus, medulla, mid brain and striatum). Each brain area was weighed and frozen until being analyzed. The brain areas were weighed and homogenized using an automatic Homogenizer (Heidolph DIAX 900, Germany) in 4 ml of ice-cold PBS (50 mM, pH 7.4). The homogenate was centrifuged at 8000 rpm for 15 min, at 4 °C using a high-speed cooling centrifuge (VS-18000 M small size, high speed, refrigerated centrifuge, Korea) the clear supernatant was separated and used for further analysis.

2.4.4. Distribution of TQ in different brain areas

The chromatographic identification of TQ was carried out at room temperature (25 ± 1) °C. The mobile phase consisted of methanol, acetonitrile, and potassium dihydrogen phosphate buffer (20 mM, pH 4.5) in the ratio of 50: 30: 20 v/v/v, which was delivered isocratically at a flow rate of 1 ml/min by c18 column (25 cm × 4.6 cm) of the HPLC system (YL 9100 HPLC, USA).

2.4.5. Determination of oxidative and non-oxidative stress parameters

2.4.5.1. Glutatione-s-transferase (GST) activity. GST activity was measured according to the method of Habig et al. [26]. Briefly, 0.4 ml potassium phosphate buffer (50 mM; pH 6.5), 0.1 ml of supernatant, 1.2 ml water and 0.1 ml CDNB (30 mM) were mixed and left in a water bath at 37 °C for 10 min. After incubation of the mixture, 0.1 ml of reduced glutathione (30 mM) was added. The difference in absorbance was determined at 340 nm using a spectrophotometer (Jenway UV-6420; Barloworld scientific, Essex, UK) at one min intervals.

2.4.5.2. Determination of reduced glutathione (GSH) levels. The assay of reduced glutathione levels was performed using Biodiagnostic kit No. GR 25 11, according to the method of Ellman (1959), 2-Nitro-s-mercaptobenzoic acid is the product of the reduction of Ellman's reagent by the SH group of GST [27]. The absorbance of the yellow-color nitromercaptobenzoic acid anion was measured spectrophotometrically (Jenway UV-6420; Barloworld scientific, Essex, UK) at 412 nm.

2.4.5.3. Determination of lipid peroxidation levels. MDA, a measure of lipid peroxidation, was measured according to the method of Ruiz-Larreaet al. [28] by determining the thiobarbituric acid-reactive substances. In this method, the thiobarbituric acid reactive substances interact with thiobarbituric acid to form a pink colored complex. The absorbance of the formed complex was read at 532 nm using the spectrophotometer (Jenway UV-6420; Barloworld scientific, Essex, UK).

2.4.5.4. Determination of Nitric Oxide (NO) levels. The assay of nitric oxide was carried out using Biodiagnostic kit No. NO 25 33. According to Moshage *et al.* [29], the NO levels were measured as nitrite using Griess reagent. In brief, when Griess reagent was added to the tissue supernatant, the nitrite changed to a deep purple azo compound which absorbance was measured using a spectrophotometer (Jenway UV-6420; Barloworld scientific, Essex, UK) at 450 nm.

2.5. Statistical analysis

All data were analyzed using Statistical Package for Social Sciences (SPSS) software (version 19). Results were expressed as mean ± standard error. Results were analyzed using Analysis of Variance (ANOVA) test. Differences were considered significant for p-value, $p < 0.05$. The percentage difference which represents the percent of change in the value in comparison with control was also evaluated.

$$\%Difference\,(\%D) = \left(\frac{treated\ value - control\ value}{control\ value}\right) \times 100\%$$

3. Results

3.1. Physical characterization of the prepared NPs

The morphological examination of MSNs by Transmission Electron Microscopy (TEM) showed that the prepared nanoparticles were almost spherical with homogeneous size distribution of about 90 nm (Fig.1A). Also, TEM micrograph revealed that the prepared MSNs had a low aggregation with a uniform alignment of pores and symmetrical shape. Dynamic Light Scattering (DLS) measurements revealed that the mean hydrodynamic diameter of MSN-TQ (105.77 ± 9.39 nm) was slightly larger than MSNs (98.80 ± 8.39 nm) (Fig. 1B). Zeta potential results showed that the prepared MSNs had high positive zeta potential charge of 30.80 ± 2.34 mV (Fig. 1C). Loading TQ to MSNs reverted their surface's zeta potential to be −15.90 ± 1.85 mV. The optical properties of the prepared formulations were investigated using UV–Vis spectroscopy, which is one of the most commonly used techniques for nanoparticles investigations. As seen in Fig. 2A, the UV–Vis absorption spectrum of free TQ showed a sharp peak at 260 nm, while, after being loaded into MSNs, the MSN-TQ demonstrated a broad band around 250 nm. It should be mentioned that MSNs didn't show any absorption peak in this region of the spectrum. The high encapsulation efficiency of MSN-TQ (95.10 ± 3.5%, where MSNs: TQ weight ratio was 1:1) would be attributed not only to the strong electrostatic interaction between the positive MSNs and the negatively charged TQ, but also to the large surface area of MSNs pores that had the ability to host large quantities of drugs.

3.2. Release profile

The in vitro release profile of TQ from MSNs showed a rapid release at the first 5 h that might be attributed to the release of TQ from the MSNs' surface. On the other hand, the slower release at a later stage was probably due to the release of TQ from the internal pores of MSNs (Fig. 2B). As the probable interaction between Si of MSNs and oxygen of TQ led to slower and controlled release of TQ from the internal pores [30].

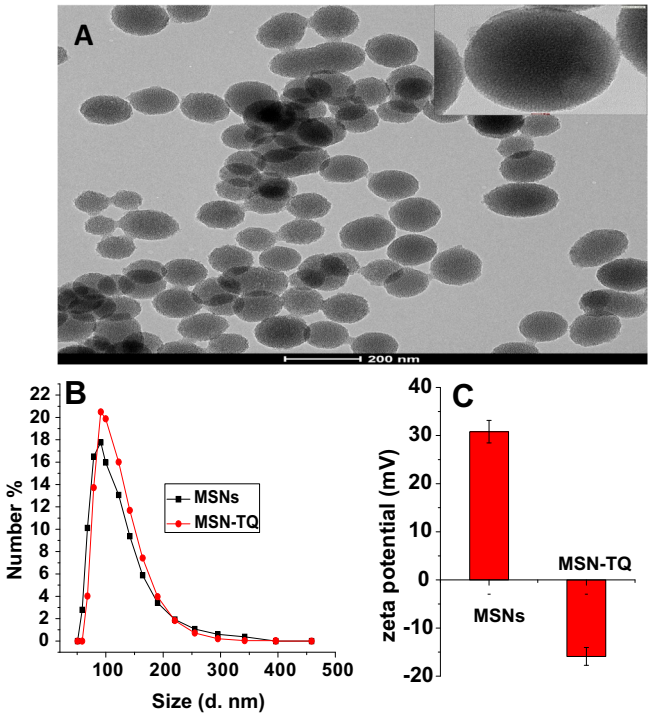

Fig. 1. (A) TEM micrograph of Mesoporous Silica Nanoparticles MSNs. (B) Particle size distribution of free and encapsulated MSNs. (C) Zeta potential distribution of MSNs and MSN-TQ, Each result represent mean ± Standard error of mean (n = 3).

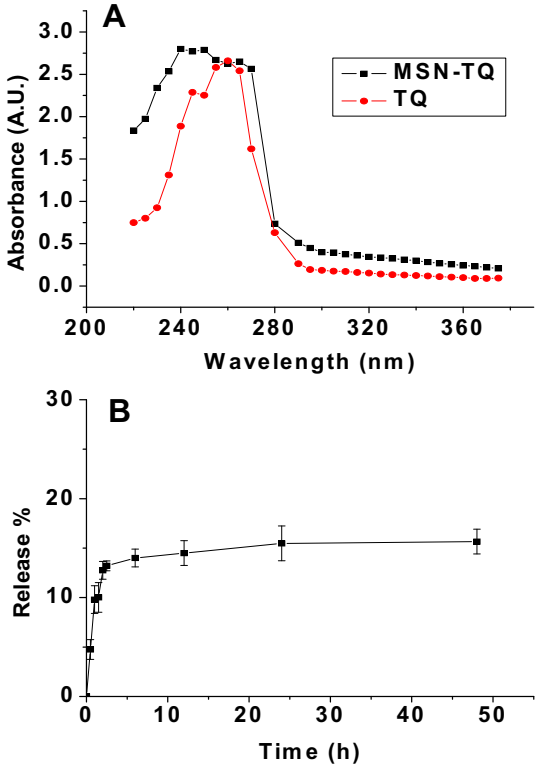

Fig. 2. (A) The absorption spectra of free TQ and MSN-TQ.(B) In vitro release profile of free TQ form TQ-loaded MSNs, Each result represent mean ± Standard error of mean (n = 3).

Table 1
The distribution of TQ in brain areas of different experimental groups.

Brain areas	TQ– group TQ concentration (μg/g tissue)	MSN-TQ group TQ concentration (μg/g tissue)	(%D)
Cortex	15.70 ± 0.79	17.78 ± 0.40	(13%)
Medulla	0.23 ± 0.05	0.24 ± 0.01	–
Cerebellum	5.08 ± 0.03	4.08 ± 0.00	(−20%)
Thalamus	401.00 ± 39.23	453.80 ± 20.21	(11%)
Striatum	165.10 ± 8.81	165.00 ± 12.04	–
Midbrain	91.76 ± 1.29	110.00 ± 1.50	(20%)
Hypothalamus	12.32 ± 0.40	21.04 ± 1.06	(71%)
Hippocampus	Zero	Zero	–

Values represent the mean ± Standard error of Mean (n = 6). %D: is the percentage difference in comparison to free TQ group and is shown only for significantly ($p < 0.05$) different means.

3.3. In vivo studies

3.3.1. The distribution of TQ in different brain areas

Table 1 demonstrates the quantitative distribution of TQ in different brain areas for two experimental groups of rats: (a) TQ-group: administrated by free TQ, (b) MSN-TQ group: administrated by MSNs-TQ. Results showed that loading of TQ to the MSNs enhanced the drug targeting to the cortex, thalamus, midbrain and hypothalamus by 13%, 11%, 20%, and 71%, respectively, as compared to the TQ-group. In contrast, the encapsulation of TQ to mesopores silica nanocarriers reduced its targeting to the cerebellum by 20%. In case of medulla, striatum, and hippocampus, there were non-significant changes in the TQ concentrations between the two experimental groups. Meanwhile, neither the free TQ nor the encapsulated one reached the hippocampus.

3.3.2. The oxidative stress parameters in different brain areas

Oxidative stress is defined as an imbalance between the generation of free radicals and the neutralization of their toxic effect by antioxidants. Fig. 3 (A-D) presents the levels of NO, MDA and GSH and the activity of GST in different brain areas for animals administrated with saline, MSNs, free TQ or MSNs-TQ.

In the cortex, the levels of NO significantly decreased for MSNs group and MSNs-TQ group by (−36%) and (−39%), respectively, compared with the control group. Meanwhile, the NO levels in the free TQ and the control groups revealed non-significant changes. The cortical GST activity significantly increased for MSNs group, free TQ group and MSNs-TQ group by 38%, 45% and 21%, respectively, above the control values. Moreover, the GST activity significantly decreased for MSNs-TQ group (9.44 ± 0.21) when compared to that of the MSNs group (10.82 ± 0.60) and the TQ group (11.33 ± 0.41). The cortical MDA levels showed significant decrease in the MSNs group 35% and the MSNs-TQ group 34% below the control levels. However, there was a significant increase in the cortical MDA levels in the free TQ group 64% relative to the control group. For the free TQ group, there was a significant increase in cortical MDA levels (12.94 ± 0.89) when compared to the MSNs (5.10 ± 0.0.37) and MSNs-TQ (5.20 ± 0.74) groups. Meanwhile, the cortical GSH levels showed non-significant changes among all experimental groups.

Regarding the medulla, the NO levels significantly decreased in the MSNs group by about 37% below the control levels. Meanwhile, NO levels demonstrated significant increases for the MSNs-TQ group 38% above the control values. However, the TQ group showed non-significant alteration in the NO levels compared to the control group. There was no-significant change in the GST activity in the MSNs group when compared to the control group. On the other hand, GST activities significantly increased in the TQ and MSNs-TQ groups by (65% and 62% respectively) above the control values. In MSNs group, GST activity (6.64 ± 0.65) showed a significant decrease in comparison with TQ (13.26 ± 0.19) and MSNs-TQ (13.00 ± 0.50) groups. The MDA

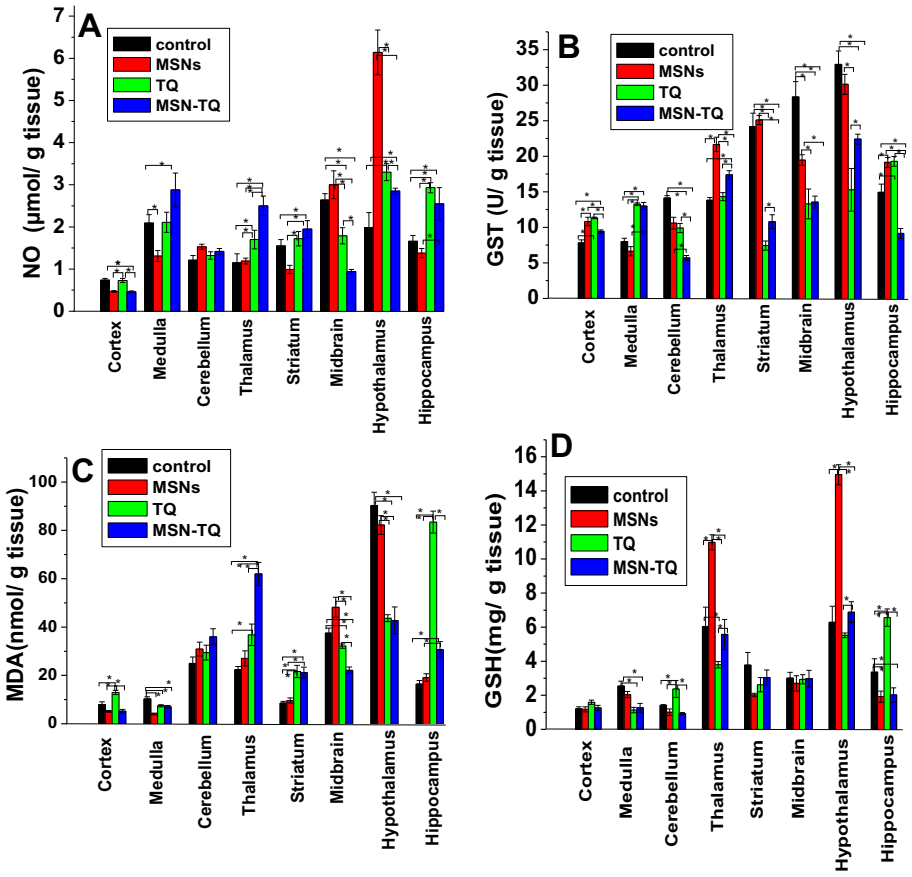

Fig. 3. A comparison of the levels of (A) NO, (B) GST, (C) MDA and (D) GSH in different brain areas for control, MSNs, free TQ and MSN-TQ groups. Each result represent mean ± Standard error of mean (n = 6). Differences were considered significant for $p < 0.05$ and labeled with *.

levels showed a significant decrease of about 61%, in the MSNs group below the control levels. But no significant changes were recorded in the case of TQ and MSNs-TQ groups relative to the control group. In addition, MDA levels in the MSNs group (4.04 ± 0.36) showed significant decrease as compared to the TQ group (7.45 ± 0.43) and the MSNs-TQ group (7.01 ± 0.54). With reference to the control group, the GSH level was not significantly changed in the MSNs group. In contrast GST levels were significantly decreased in the TQ group and MSNs-TQ group by 51% and 50%, respectively, below the control values.

The results of oxidative stress parameters for the cerebellum showed that there were non-significant changes in the cerebellar NO and MDA levels among all experimental groups. Moreover, the GST activity was significantly decreased in MSNs group, TQ group and MSNs-TQ group by 25%, 30% and 60%, respectively, as compared to the control group. GSH was significantly increased in the TQ group 68% relative to the control group. In addition, its levels were significantly decreased in the MSNs and MSNs-TQ groups to (1.01 ± 0.19) and (0.92 ± 0.07) respectively, relative to the TQ group (2.37 ± 0.49).

For the thalamus area, the NO levels for the MSNs group recorded non-significant changes from the control group, while, it was significantly increased in the TQ group by 48% and MSNs-TQ group by117% above the control values. In addition, the NO levels were significantly decreased in the MSNs group (1.19 ± 0.07) and in the TQ group (1.70 ± 0.22) with reference to the MSNs-TQ group (2.5 ± 0.23). Also, the GST activity showed non-significant changes in the TQ group, but, significantly increased in the MSNs group by 60% and in the MSNs-TQ group by 26% above the control group. It is worth to mention here that the GST activity in the thalamus of the MSNs group (21.67 ± 1.01) was significantly higher than that of TQ group (14.32 ± 0.57) and MSNs-TQ group (17.40 ± 0.58). MDA level recorded non-significant change in the MSNs group, however, it was significantly increased in the TQ group by 65% besides that MSNs-TQ group by 177% above the control values. Regarding the GSH levels in the thalamus, there was non-significant change in the GSH levels in the MSNs-TQ group as compared to the control group. Meanwhile, the GSH level recorded a significant increase by 82% in the MSNs group and a significant decrease 38% in the TQ group when compared to the control levels. The GSH level was significantly increased in the MSNs group (10.98 ± 0.45) relative to the TQ group (3.79 ± 0.19) and the MSNs-TQ group (5.57 ± 0.88).

The NO levels in the striatum showed non-significant changes in the MSNs group and the TQ group as compared to the control group. Moreover, NO levels significantly increased in MSNs-TQ group above the control group by 26%. The GST activity was significantly decreased below the control by 69% in the TQ group and by 55% in the MSNs-TQ group. Meanwhile, a non-significant change in the GST activity was recorded in the MSNs group when compared to the control group. The activity of the GST was significantly increased in the MSNs group (25.10 ± 0.65) as compared to the TQ (7.44 ± 0.64) and MSNs-TQ (10.80 ± 0.98) groups. Regarding the MDA levels in the striatum, they were non-significantly alternated in the MSNs group, while, TQ group and the MSN - TQ group showed significant increases by about 153% and 148% above the control values. The GSH levels in the striatum were significantly decreased in the MSNs group by 46% and also in the TQ group by 31% below the control values. At the same time, GSH levels in the striatum of MSNs group recorded non-significant changes relative to the control group. It is worth to mention here, that non-significant changes in the striatum GSH levels were detected among the MSNs, TQ and MSNs-TQ groups.

In the midbrain, significant decreases in the NO levels were obtained in the TQ group by 32% and in the MSNs-TQ group 64% as compared to the control group levels. Meanwhile, the MSNs group recorded non-significant alterations in the NO levels in the midbrain relative to the control group. The activity of GST in the midbrain was significantly decreased in the MSNs, TQ and MSNs-TQ groups by (31%, 53% and 52%, respectively) when compared to the control group. The GST activity recorded a significant increase in the MSNs group (19.47 ± 0.75) as compared to the TQ (13.30 ± 2.10) and MSNs-TQ (13.56 ± 0.83) groups. MDA levels in the midbrain were significantly increased in the MSNs group 28% above the control, but, in the TQ and MSNs-TQ groups, the MDA levels were significantly decreased by (14% and 41%, respectively) below the control levels. Moreover, MDA levels in the midbrain of the MSNs group were significantly higher (48.21 ± 4.09) than those for the TQ (32.14 ± 0.91) and MSNs-TQ (22.10 ± 1.37) groups. Finally, non-significant changes in the GSH levels in the midbrain were recorded among all experimental groups.

In the hypothalamus, the NO levels showed non-significant changes in the TQ and MSNs-TQ groups as compared to the control group. However, NO levels were significantly increased in the MSNs group by 209% above the control levels. The GST activity in the hypothalamus was not significantly altered in MSNs group, but, in case of the TQ and MSNs-TQ groups, it was significantly decreased by (54% and 33%, respectively) below the control group. Non-significant change was recorded in the MDA level in the MSNs group in comparison to the control group. At the same time, MDA levels were significantly decreased in the TQ and MSNs-TQ groups by 52% and 53%, respectively below the control group. In the hypothalamus, the GSH levels showed non-significant changes in TQ and MSNs-TQ groups, but it was significantly increased in the MSNs group by 138% above the control levels. The increase in the GSH levels in the hypothalamus of the MSNs (14.95 ± 0.59) group was also significant in comparison to TQ (5.52 ± 0.14) and MSNs-TQ (6.88 ± 0.61) groups.

For the hippocampus, the NO levels were significantly increased in the TQ and MSNs-TQ groups by 44% and 54%, respectively above the control. Meanwhile, non-significant change in the NO levels was depicted in the MSNs group as compared to the control group. The levels of NO were significantly reduced in the MSNs group (1.38 ± 0.11) as compared to the TQ (2.39 ± 0.11) and MSNS-TQ (2.55 ± 0.38) groups. The hippocampal GST activity showed a significant increase in the MSNs group by 28% and in the TQ group by 29%above the control. In contrast, there was a significant decrease recorded in the MSNs-TQ group 39% below the control. The decrease in the hippocampal GST activity in the in MSNs-TQ group (9.15 ± 0.70) was also significant compared to that of the MSNs (19.14 ± 0.69) and TQ (19.28 ± 0.69) groups. The MDA level in the hippocampus didn't show any significant change in the MSNs group, but, it was significantly increased by 409% in the TQ group and by 87% in the MSNs-TQ group above the control levels. The change in the hippocampal MDA levels in the TQ (83.44 ± 4.54) group was significantly higher than those in the MSNs (19.12 ± 1.55) and MSNs-TQ (30.63 ± 3.34) groups. Hippocampal GSH levels recorded significant decreases in the MSNs group by 43% and in the MSNs-TQ group by 39% relative to the control group. Meanwhile, the GSH level recorded a significant increase in the TQ group 95% as compared to the control group. The hippocampal GSH levels in the TQ group (6.56 ± 0.51) were significantly higher than those for the MSNs group (1.92 ± 0.33) and the MSNs-TQ group (2.02 ± 0.42).

4. Discussion

Blood brain barrier (BBB) acts as the best gatekeeper in the body for any exogenous materials due to the presence of the tight endothelial barrier which prevents pharmaceuticals from penetrating the barrier [31]. Scientists made several trials to overcome this challenge. One of these attempts was using nanoparticles as a drug delivery system. Previous studies reported that MSNs could cross the BBB and reach the brain by the endocytosis mechanism or with other specific transporters [32–34]. The mechanism by which silica nanoparticles can cross the BBB depends on physicochemical properties such as particle size and zeta potential [35]. So, the shape, charge and size MSNs are the key parameters in determining their validity as brain drug delivery systems.

Transmission Electron Microscope (TEM) investigation showed that MSNs was successfully synthesized with homogenous shape and size. This was also confirmed by DLS measurements which revealed that the mean hydrodynamic diameter of the MSNs-TQ was slightly larger than the free MSNs. This increase in size might be attributed to the attachment and encapsulation of TQ to the pores of the MSNs. The polydispersity Index (PDI) describes the degree of uniformity and homogeneity of the particle size distribution. PDI values ranging from 0.1 to 0.5 point to a narrow size distribution, while a PDI higher than 0.5 indicates a broad distribution [36]. In the present study, the PDI values of free MSNs (0.186) and MSN-TQ (0.4) both indicated a narrow and homogenous distribution of the prepared formulations. It is well known that the drug delivery systems must have a small PDI value in order to enhance their pharmacokinetic parameters, (e.g. absorbance and distribution) [37].The inversion of the zeta potential charge of MSN-TQ was probably attributed to the encapsulation of the negatively charged TQ molecules [21]. This value of zeta potential indicated intermediate stability of MSN-TQ. One of the proposed suggestions for a future work is to coat the prepared formulation with a charged polymer, in order to increase its zeta potential and hence, its stability. The loading efficiency of TQ at MSNs was better than the other previously tested Nano-carriers. For example, previously reported Chitosan loading efficiency of TQ was 63.30 ± 3.50% [21], whereas that for solid lipid nanoparticles was 84.49 ± 3.36 [38], and the loading efficiency of Poly Dl-Lactide-*Co*-Glycolide (PLGA) for TQ was found to be 62% [39]. The probable interaction between Si of MSNs and oxygen of TQ led to slower and controlled release of TQ from the internal pores [40]. The present in vitro release profile of TQ from MSNs was in line with that of the release of curcumin from MSNs described in the study of Jambhrunkar et al. [41]. Physical characterization assessments showed that the prepared MSNs were ideal brain drug delivery and targeting systems because of their appropriate particle size, which enabled them to stay in the blood stream for a long time, escape from the immune system and pass through the BBB [42].

The TQ distribution results revealed that loading TQ on MSNPs led to a change in the map of TQ distribution throughout different regions of the brain as it resulted in increased drug access to cortex, thalamus, midbrain and hypothalamus. This enabled to target medications to certain areas of the brain. This drug bio-distribution was also expected to change with other types of drug carriers with different shapes and sizes. This is one main recommendation for future studies based on the results of the present work.

Lipid peroxidation is one of the major manifestations of oxidative damage and has been found to play an important role in toxicity [43]. NO is a Neuro-modulatory agent having a role in the CNS. The pharmacological manipulation of NO pathway may open a new treatment approach of various neuropsychiatric disorders [44], however, it has been shown that NO has contradictory roles in cellular systems such as being an oxidant at high levels and antioxidant at low levels [45,46].

In rat groups administrated with MSNs and MSNs-TQ, the cortical MDA and NO levels were significantly decreased below the control values. It has been shown that the reduction in NO levels reduces the production of the peroxynitite, which causes a decrease in tissue peroxidation and quenches the formation of the MDA [47]. GSH is a major endogenous antioxidant having an important role in repairing DNA and regulating a wide range of metabolic processes [48]. GST is an enzyme belonging to the GSH mediated enzyme and defense system, helping the sulfur atom in the GSH to connect with toxic materials [49]. In the free MSNs, TQ and MSNs-TQ groups, there were non-significant changes in the cortical GSH levels concomitant with a significant increase in the

cortical GST activity as compared to the control group. This significant increase in the cortical GST activity might be a kind of protective mechanism from the cortex toward a slight induced-oxidative stress due to the entrance of any exogenous agent [49].

The medullary NO and MDA levels were also declined in the free MSNs group, but without any significant changes in the GSH levels or the GST activity. Fortunately, it is clear from the present data that free MSNs enhance the antioxidant system in the medulla. The TQ group expressed a significant increase in the cortical GST activity (as compared to all the experimental groups) as a protective action to the cells against the significant increase in the MDA levels [50]. Loading TQ in MSNs significantly reduced the MDA levels below those obtained due to free TQ and thus, helped in relieving the induced oxidative stress. There was a non-significant change in the amount of free and encapsulated TQ reaching the medulla and this was reflected in the non-significant changes in MDA, GSH level in addition to the activity of GST in the TQ and MSNs-TQ groups. However, the two groups showed a significant increase in the GST and a significant decrease in the GSH as compared to the control group. In general, GSH is an antioxidant and its function is the detoxification of endogenous and exogenous toxic compounds by changing their solubility, so, that the decrease in the GSH levels may be due to its consumption in the protection of cells from the generated free radicals [51]. Supporting this suggestion, the increase in the GST level in the medulla may be considered as an indication of cellular stress response to oxidative stress [52]. In the medulla, in the case of the MSNs - TQ group, the levels of NO were significantly increased concomitant with significant decreases in MDA levels. Kanner et al. [53] suggested that the increase in NO levels could prevent the generation of lipid peroxidation by working as electron donor, quenching the production of free radicals, and thus, decreasing MDA levels and helping them to return to their normal values.

The levels of cerebellar GST in the MSNs group were significantly decreased. This may be due to its consumption in overcoming the resulting oxidative stress [54]. In the free TQ group there was a significant decrease in the cerebellar GST activity with a significant increase in GSH levels. The observed significant decrease in GST activity may be due to its exhaustion in turning the GSH to an oxidized form to affront the induced oxidative stress [55,56].

In the thalamus of rats that were injected with MSNs, the increase in the levels of GST enzyme and GSH antioxidant was an evidence of induced-oxidative stress and an attempt from the cells to be protected against it [57]. In the thalamus of the TQ group, the reduction in GSH levels may be due to its depletion in restoring the levels of MDA and NO to their normal levels by cleaning up the resultant free radicals [58]. In the thalamus, the group of MSNs-TQ showed further oxidative stress and more damage as compared to the free TQ group. This was evident from the higher levels of MDA and NO, in addition to elevated levels of GST in order to defense these induced ROS. This additional oxidative stress may be due to the increase in the amount of TQ that entered the brain area using the MSNs as a nano-carrier. It is worth to mention here, that the encapsulation of TQ in MSNs improved its delivery to the thalamus, but, unfortunately, failed to protect the thalamus from the induced-oxidative stress caused by the increase in the TQ concentration.

In the striatum, the group injected with MSNs showed a significant decrease in the GSH level as compared to the control group, this GSH decrease may be an indication of slight oxidative stress [48]. In the TQ and MSNs-TQ groups, GST activity and GSH levels were decreased, which resulted in less clearance of the lipid peroxidation and toxic aldehydes and as a consequence, the levels of MDA in the striatum were increased [59]. Since the amount of TQ which reached the brain either in the free form or in the encapsulated form was nearly the same, there were non-significant changes in the oxidative stress parameters between the free TQ and MSNs-TQ groups.

The midbrain of the MSNs group in addition to the striatum of TQ and MSNs-TQ groups exhibited a slight significant increase in MDA levels above the normal level that might refer to the decrease in the activity of GST. For the free TQ group in the midbrain, TQ acts as an antioxidant [60], helping in reducing the levels of NO and MDA by reducing the free radicals. It is reported that the GST activity significantly decreased due to its action as an antioxidative stress enzyme [47]. Moreover, in the midbarin, in the case of the MSNs - TQ group, further antioxidant activity was shown due to the significant increase of the amount of TQ that reached the midbrain upon its encapsulation in MSNs. This means that the encapsulation of TQ in the MSNs increases its antioxidant activity due to the regular release of the nanoparticles as well as the reduction of the oxidation effect of free MSNs in the midbrain.

In the hypothalamus, the levels GSH and the activity of GST in the free thymoquinone group deceased because of their consumption in the reduction of MDA level showing antioxidative stress activity of TQ in the brain hypothalamus. In the case of MSNs-TQ group, hypothalamus area, there were non-significant changes in No, MDA and GSH levels as compared to the free TQ group, however, the activity of GST was higher meaning that its consumption was less than the free TQ group due to less damage in the cell. The oxidative stress results of the thalamus showed that TQ was acting as an antioxidant and that its encapsulation helped in protecting the hypothalamus from the oxidative stress.

Although HPLC didn't detect the TQ in the hippocampus of the rat brain, there were significant changes in the oxidative stress parameters measured in this brain area. In the hippocampus, the group of MSNs showed a significant decrease in the levels of GSH, which was catalyzed by the GST enzyme to restore NO and MDA to their normal levels [55]. In the hippocampus of the TQ group, the observed activity of GST and GSH levels were increased to protect this brain area from massive increases in MDA and No [49]. It is well known that the hippocampus area is sensitive to lipid peroxidation due to its high level of iron and polyunsaturated fatty acids [61]. The encapsulation of TQ in MSNs nanoparticles significantly decreased the MDA levels and thus, protecting the hippocampus from oxidative stress damage.

5. Conclusion

Here, we introduce MSNs as a smart nanoplatform that can be used for targeting drug to certain brain areas. The prepared formulation was characterized using different physical techniques and it was found that its properties were suitable for drug delivery applications. The MSNs prepared in the present study were in the range of 90 nm, spherical in shape and had the ability to cross the BBB. Assessing the bio-distribution of TQ through different brain areas demonstrated that the brain areas behaved differently in their uptake and response (as evaluated through the measurement of oxidative stress parameters) to TQ upon encapsulation in MSNs. The knowledge gained in this study would open the door for adopting MSNs as a viable strategy for targeting drugs to different brain areas for many therapeutic and diagnostic applications.

References

[1] M. Stützle, J. Flamm, S. Carle, K.S.-A., U. DMPK, Nose-to-brain Delivery of Insulin for Alzheimer's Disease, Hrcak.Srce.Hr . (n.d.) https://hrcak.srce.hr/index.php?show=clanak&id_clanak_jezik=212872, (2015) , Accessed date: 11 September 2018.

[2] A. Chaudhary, U. Nagaich, N. Gulati, ... V.S.-J.A.P.E., undefined, Enhancement of Solubilization and Bioavailability of Poorly Soluble Drugs by Physical and Chemical Modifications: A Recent Review, Academia.Edu, 2012 (n.d.), http://www.academia.edu/download/31631939/solubility.pdf , Accessed date: 11 September 2018.

[3] S.S.- Fitoterapia, Undefined 2010, Applications of Novel Drug Delivery System for Herbal Formulations, Elsevier. (n.d.). https://www.sciencedirect.com/science/article/pii/S0367326X10000912 (accessed September 11, 2018).

[4] J. Jorge, M. Verelst, G. R. D. Gastro, M. A. Utrera Martines, Synthesis parameters for control of mesoporous silica nanoparticles (MSNs), Biointerface Research in Applied Chemistry. 1520–1524.

[5] F. Tang, L. Li, D. Chen, Mesoporous silica nanoparticles: synthesis, biocompatibility and drug delivery, Adv. Mater. 24 (2012) 1504–1534, https://doi.org/10.1002/adma.201104763.

[6] I. Slowing, J. Vivero-Escoto, … C.W.-A. drug delivery, undefined 2008, Mesoporous Silica Nanoparticles as Controlled Release Drug Delivery and Gene Transfection Carriers, Elsevier. (n.d.). https://www.sciencedirect.com/science/article/pii/S0169409X08000951 (accessed September 11, 2018).

[7] L. Rashidi, … E.V.-F.-I.J. of, undefined 2013, Mesoporous Silica Nanoparticles as a Nanocarrier for Delivery of Vitamin C, Ijbiotech.Com. (n.d.). http://www.ijbiotech.com/article_7211_0.html (accessed September 11, 2018).

[8] H. Baghirov, D. Karaman, T. Viitala, A. Duchanoy, Y.-R. Lou, V. Mamaeva, E. Pryazhnikov, L. Khiroug, C. de Lange Davies, C. Sahlgren, J.M. Rosenholm, Feasibility study of the permeability and uptake of mesoporous silica nanoparticles across the blood-brain barrier, PLoS One 11 (2016) e0160705, , https://doi.org/10.1371/journal.pone.0160705.

[9] M. El–Dakhakhny, Studies on the chemical constitution of Egyptian *Nigella sativa* L. seeds. II 1 the essential oil, Planta Med. 11 (1963) 465–470, https://doi.org/10.1055/s-0028-1100266.

[10] M.A. Mansour, M.N. Nagi, A.S. El-Khatib, A.M. Al-Bekairi, Effects of thymoquinone on antioxidant enzyme activities, lipid peroxidation and DT-diaphorase in different tissues of mice: a possible mechanism of action, Cell Biochem. Funct. 20 (2002) 143–151, https://doi.org/10.1002/cbf.968.

[11] S. Umar, J. Zargan, K. Umar, S. Ahmad, … C.K.-C., Undefined 2012, Modulation of the Oxidative Stress and Inflammatory Cytokine Response by Thymoquinone in the Collagen Induced Arthritis in Wistar Rats, Elsevier. (n.d.). https://www.sciencedirect.com/science/article/pii/S0009279712000336 (accessed September 11, 2018).

[12] A.A. Al-Majed, F.A. Al-Omar, M.N. Nagi, Neuroprotective effects of thymoquinone against transient forebrain ischemia in the rat hippocampus, Eur. J. Pharmacol. 543 (1-3) (2006) 40–47.

[13] A. Alhebshi, M. Gotoh, I.S.-B., and biophysical research, undefined, Thymoquinone Protects Cultured Rat Primary Neurons Against Amyloid β-induced Neurotoxicity, Elsevier, 2013 (n.d.), https://www.sciencedirect.com/science/article/pii/S0006291X1300466X , Accessed date: 11 September 2018.

[14] H. Gali-Muhtasib, … A.R.-T. International Journal, Undefined 2006, Thymoquinone: A Promising Anti-cancer Drug From Natural Sources, Elsevier. (n.d.). https://www.sciencedirect.com/science/article/pii/S1357272505003614 (accessed September 11, 2018).

[15] C. Woo, A. Kumar, G. Sethi, K.T.-B., pharmacology, undefined, Thymoquinone: Potential Cure for Inflammatory Disorders and Cancer, Elsevier, 2012 (n.d.), https://www.sciencedirect.com/science/article/pii/S0006295211007350 , Accessed date: 11 September 2018.

[16] M.M. Abukhader, The effect of route of administration in thymoquinone toxicity in male and female rats, Indian J. Pharm. Sci. 74 (3) (2012) 195.

[17] R.J. Reiter, Oxidative processes and antioxidative defense mechanisms in the aging brain, FASEB J. 9 (1995) 526–533, https://doi.org/10.1096/fasebj.9.7.7737461.

[18] R. Pamplona, M. Portero-Otın, C. Ruiz, … R.G.-M. of ageing, undefined 2000, Double Bond Content of Phospholipids and Lipid Peroxidation Negatively Correlate With Maximum Longevity in the Heart of Mammals, Elsevier. (n.d.). https://www.sciencedirect.com/science/article/pii/S0047637499000457 (accessed September 11, 2018).

[19] D.A. Butterfield, E.R. Stadtman, Protein oxidation processes in aging brain, Advances in Cell Aging and Gerontology, 2 Elsevier, 1997, pp. 161–191.

[20] Y.M. Tsai, C.F. Chien, L.C. Lin, T.H. Tsai, Curcumin and its nano-formulation: the kinetics of tissue distribution and blood–brain barrier penetration, Int. J. Pharm. 416 (1) (2011) 331–338.

[21] S. Alam, Z. Khan, G. Mustafa, ... M.K.-I., journal, undefined, Development and Evaluation of Thymoquinone-encapsulated Chitosan Nanoparticles for Nose-to-brain Targeting: A Pharmacoscintigraphic Study, Ncbi.Nlm.Nih.Gov. (n.d.) https://www.ncbi.nlm.nih.gov/pmc/articles/PMC3497894/, (2012) , Accessed date: 11 September 2018.

[22] N. Ahmad, R. Ahmad, M. Alam, M. Samim, … Z.I.-I. journal of, undefined 2016, Quantification and Evaluation of Thymoquinone Loaded Mucoadhesive Nanoemulsion for Treatment of Cerebral Ischemia, Elsevier. (n.d.). https://www.sciencedirect.com/science/article/pii/S0141813016302434 (accessed September 11, 2018).

[23] N. Elbialy, N. Mohamed, A.M.-M. and Mesoporous, Undefined 2014, Synthesis, Characterization and Application of Gold Nanoshells Using Mesoporous Silica Core, Elsevier. (n.d.). https://www.sciencedirect.com/science/article/pii/S1387181114000572 (accessed September 11, 2018).

[24] B.F.-A., optics, undefined, Revisiting the Method of Cumulants for the Analysis of Dynamic Light-scattering Data, Osapublishing.Org, 2001 (n.d.), https://www.osapublishing.org/abstract.cfm?uri=ao-40-24-4087 , Accessed date: 11 September 2018.

[25] F. Sheikhbahaei, M. Khazaei, A. Rabzia, K. Mansouri, A. Ghanbari, Protective effects of thymoquinone against methotrexate-induced germ cell apoptosis in male mice, International Journal of Fertility & Sterility 9 (4) (2016) 541.

[26] W. Habig, M. Pabst, W.J.-J. of biological Chemistry, Undefined 1974, Glutathione S-transferases the First Enzymatic Step in Mercapturic Acid Formation, ASBMB. (n.d.). http://www.jbc.org/content/249/22/7130.short (accessed September 12, 2018).

[27] G.E.-A. of biochemistry and biophysics, undefined 1959, Tissue Sulfhydryl Groups, Researchgate.Net. (n.d.). https://www.researchgate.net/profile/Ronald_Rodriguez2/post/Would_anyone_like_to_share_the_protocol_for_the_determine_Non-protein_thiol_NPSH_content_in_plant_root_and_shoot/attachment/59d6452f79197b80779a0583/AS:452127798632448@1484807075009/download/NP-SH+protocol+Ellman+1959.pdf (accessed September 12, 2018).

[28] M. Ruiz-Larrea, A. Leal, M. Liza, M. Lacort, H. de G. Steroids, Undefined 1994, Antioxidant Effects of Estradiol and 2-hydroxyestradiol on Iron-induced Lipid Peroxidation of Rat Liver Microsomes, Elsevier. (n.d.). https://www.sciencedirect.com/science/article/pii/0039128X9490006X (accessed September 12, 2018).

[29] H. Moshage, B. Kok, … J.H.-C., Undefined 1995, Nitrite and Nitrate Determinations in Plasma: A Critical Evaluation., Clinchem.Aaccjnls.Org. (n.d.). http://clinchem.aaccjnls.org/content/41/6/892.short (accessed September 12, 2018).

[30] M. Liong, J. Lu, M. Kovochich, T. Xia, … S.R.-A., Undefined 2008, Multifunctional Inorganic Nanoparticles for Imaging, Targeting, and Drug Delivery, ACS Publ. (n.d.). https://pubs.acs.org/doi/abs/10.1021/nn800072t (accessed September 12, 2018).

[31] W.M. Pardridge, Blood–brain barrier delivery, Drug Discov. Today 12 (1) (2007) 54–61.

[32] A. Parveen, S.H.M. Rizvi, F. Mahdi, S. Tripathi, I. Ahmad, R.K. Shukla, K.K. Vinay, S. Ranjana, K.P. Devendrav, A.A. Mahdi, Silica nanoparticles mediated neuronal cell death in corpus striatum of rat brain: implication of mitochondrial, endoplasmic reticulum and oxidative stress, J. Nanopart. Res. 16 (11) (2014) 2664.

[33] A. Parveen, S.H.M. Rizvi, F. Mahdi Sushma, I. Ahmad, P.P. Singh, A.A. Mahdi, Intranasal exposure to silica nanoparticles induces alterations in pro-inflammatory environment of rat brain: involvement of oxidative stress, Toxicol. Ind. Health 33 (2) (2017) 119–132.

[34] J. Jampilek, K. Zaruba, M. Oravec, M. Kunes, P. Babula, P. Ulbrich, I. Brezaniova, B. Opatrilova, J. Triska, P. Suchy, Preparation of silica nanoparticles loaded with nootropics and their in vivo permeation through blood-brain barrier, Biomed. Res. Int. 2015 (2015).

[35] S. Honary, F. Zahir, Effect of zeta potential on the properties of nano-drug delivery systems-a review (part 2), Trop. J. Pharm. Res. 12 (2) (2013) 265–273.

[36] L. Wu, J. Zhang, W.W.-A. Drug Delivery Reviews, Undefined 2011, Physical and Chemical Stability of Drug Nanoparticles, Elsevier. (n.d.). https://www.sciencedirect.com/science/article/pii/S0169409X11000172 (accessed September 12, 2018).

[37] D. Lankveld, A. Oomen, P. Krystek, A.N., Biomaterials, undefined, The Kinetics of the Tissue Distribution of Silver Nanoparticles of Different Sizes, Elsevier, 2010 (n.d.), https://www.sciencedirect.com/science/article/pii/S0142961210008884 , Accessed date: 12 September 2018.

[38] R. Surekha, V. Aishwarya, H. Sumathi, Thymoquinone loaded solid lipid nanoparticle: formation, characterization and in vitro cell viability assay, Int J Pharm. Bio. Sci 6 (1) (2015) 449–464.

[39] I. Nallamuthu, A. Parthasarathi, & F. Khanum. (2013). Thymoquinone-loaded PLGA nanoparticles: antioxidant and anti-microbial properties.

[40] M. Liong, J. Lu, M. Kovochich, T. Xia, S.G. Ruehm, A.E. Nel, F. Tamanoi, J.I. Zink, Multifunctional inorganic nanoparticles for imaging, targeting, and drug delivery, ACS Nano 2 (5) (2008) 889–896.

[41] S. Jambhrunkar, S. Karmakar, A. Popat, M. Yu, C.Y.-R. Advances, Undefined 2014, Mesoporous Silica Nanoparticles Enhance the Cytotoxicity of Curcumin, Pubs.Rsc.Org. (n.d.). http://pubs.rsc.org/en/content/articlehtml/2013/ra/c3ra44257h (accessed September 12, 2018).

[42] S. Li, Z. Ji, M. Zou, X. Nie, Y. Shi, G. Cheng, Preparation, characterization, pharmacokinetics and tissue distribution of solid lipid nanoparticles loaded with tetrandrine, AAPS PharmSciTech 12 (2011) 1011–1018, https://doi.org/10.1208/s12249-011-9665-3.

[43] R. Anane, E.E. Creppy, Lipid peroxidation as pathway of aluminium cytotoxicity in human skin fibroblast cultures: prevention by superoxide dismutase+ catalase and vitamins E and C, Human & Experimental Toxicology 20 (9) (2001) 477–481.

[44] A. Ray, A. Chakraborti, K. Gulati, Current trends in nitric oxide research, Cellular and Molecular Biology (Noisy-le-Grand, France) 53 (1) (2007) 3–14.

[45] E. Fadillioglu, H. Erdogan, M. Iraz, M. Yagmurca, Effects of caffeic acid phenethyl ester against doxorubicin-induced neuronal oxidant injury, Neurosci. Res. Commun. 33 (2) (2003) 132–138.

[46] A. Ilhan, O. Akyol, A. Gurel, F. Armutcu, M. Iraz, E. Oztas, Protective effects of caffeic acid phenethyl ester against experimental allergic encephalomyelitis-induced oxidative stress in rats, Free Radic. Biol. Med. 37 (3) (2004) 386–394.

[47] İ. Gülşen, H. Ak, N. Çölçimen, H. Alp, M.A.-W. Neurosurgery, Undefined 2016, Neuroprotective Effects of Thymoquinone on the Hippocampus in a Rat Model of Traumatic Brain Injury, Elsevier. (n.d.). https://www.sciencedirect.com/science/article/pii/S1878875015012152 (accessed September 12, 2018).

[48] G. Joshi, C. Aluise, M. Cole, R. Sultana, W.P.- Neuroscience, Undefined 2010, Alterations in Brain Antioxidant Enzymes and Redox Proteomic Identification of Oxidized Brain Proteins Induced by the Anti-cancer Drug Adriamycin: Implications, Elsevier. (n.d.). https://www.sciencedirect.com/science/article/pii/S0306452210000692 (accessed September 12, 2018).

[49] J.D. Hayes, J.U. Flanagan, I.R. Jowsey, Glutathione transferases, Annu. Rev. Pharmacol. Toxicol. 45 (2005) 51–88, https://doi.org/10.1146/annurev.pharmtox.45.120403.095857.

[50] W.H. Habig, Glutathione S-transferase (rat and human), Methods Enzymol. 77 (1981) 218–231.

[51] A.P. Mazzetti, M.C. Fiorile, A. Primavera, M.L. Bello, Glutathione transferases and neurodegenerative diseases, Neurochem. Int. 82 (2015) 10–18.

[52] V. Calabrese, D. E. B. R. A. Boyd-Kimball, G. Scapagnini, & D. A. Butterfield. (2004). Nitric oxide and cellular stress response in brain aging and neurodegenerative disorders: the role of vitagenes. In vivo, 18(3), 245–268.

[53] J. Kanner, S. Harel, R. Granit, Nitric oxide, an inhibitor of lipid oxidation by lipoxygenase, cyclooxygenase and hemoglobin, Lipids 27 (1) (1992).

[54] S.A. Noeman, H.E. Hamooda, A.A. Baalash, Biochemical study of oxidative stress markers in the liver, kidney and heart of high fat diet induced obesity in rats, Diabetol. Metab. Syndr. 3 (2011) 17, https://doi.org/10.1186/1758-5996-3-17.

[55] L. Yuan, F. Chen, L. Ling, H. Bo, … Z.C.-J. of P., Undefined 2008, Protective Effects of Total Flavonoids of *Bidens bipinnata* L. Against Carbon Tetrachloride-induced Liver Fibrosis in Rats, Wiley Online Libr. (n.d.). https://onlinelibrary.wiley.com/

doi/abs/10.1211/jpp.60.10.0016 (accessed September 12, 2018).
[56] G. Joshi, C.D. Aluise, M.P. Cole, R. Sultana, W.M. Pierce, M. Vore, D.K. St Clair, D.A. Butterfield, Alterations in brain antioxidant enzymes and redox proteomic identification of oxidized brain proteins induced by the anti-cancer drug adriamycin: implications for oxidative stress-mediated chemobrain, Neuroscience 166 (3) (2010) 796–807.
[57] S. K. R. Zaidi, T. M. Al-Qirim, & N. Banu. (2005). Effects of antioxidant vitamins on glutathione depletion and lipid peroxidation induced by restraint stress in the rat liver. Drugs in R & D, 6(3), 157–165.
[58] Y.A. Khadrawy, I.M. Mourad, H.S. Mohammed, N.A. Noor, E.H. Aboul, Cerebellar neurochemical and histopathological changes in rat model of Parkinson's disease induced by intrastriatal injection of rotenone, Gen. Physiol. Biophys. 36 (1) (2017) 99–108.
[59] J. Samson, R. Sheeladevi, R.R.- Neurotoxicology, Undefined 2007, Oxidative Stress in Brain and Antioxidant Activity of *Ocimum sanctum* in Noise Exposure, Elsevier. (n.d.). https://www.sciencedirect.com/science/article/pii/S0161813X07000472 (accessed September 12, 2018).
[60] M.A. Mansour, M.N. Nagi, A.S. El-Khatib, A.M. Al-Bekairi, Effects of thymoquinone on antioxidant enzyme activities, lipid peroxidation and DT-diaphorase in different tissues of mice: a possible mechanism of action, Cell Biochem. Funct. 20 (2) (2002) 143–151.
[61] B. Halliwell, J. Gutteridge, Free Radicals in Biology and Medicine 2015. (n.d.). https://www.google.com/books?hl=ar&lr=&id=3DlKCgAAQBAJ&oi=fnd&pg=PP1&dq=Halliwell,+B.,+%26+Gutteridge,+J.+M.+(2007).+Free+radicals+in+biology+and+medicine.+Oxford+University+Press,+USA.&ots=bokGbWCrk_&sig=0pG0XEzUH5nG0J2VV_vZT4lowRY ((accessed September 12, 2018)).